Sensitive SERS nanotags for use with a hand-held 1064 nm Raman Spectrometer

Hayleigh Kearns,[a] Fatima Ali, [a] Matthew A. Bedics, [b] Neil C. Shand, [c] Karen Faulds, [a] Michael R. Detty, [b] and Duncan Graham [a] *

[a] Department of Pure and Applied Chemistry, Technology and Innovation Centre, University of Strathclyde, 99 George Street, Glasgow, G1 1RD, United Kingdom; Email: duncan.graham@strath.ac.uk

[b] Department of Chemistry, University at Buffalo, The State University of New York, New York 14260, United States

[c] Dstl, Porton Down, Salisbury, Wiltshire, SP4 0JQ, United Kingdom

Abstract

This is the first report of the use of a hand-held 1064 nm Raman spectrometer combined with red shifted surface enhanced Raman scattering (SERS) nanotags to provide an unprecedented performance in the short-wave infrared (SWIR) region. A library consisting of 17 chalcogenopyrylium nanotags produce extraordinary SERS responses with femtomolar detection limits being obtained using the portable instrument. This is well beyond previous SERS detection limits at this far red shifted wavelength and opens up new options for SERS sensors in the SWIR region of the electromagnetic spectrum (between 950-1700 nm).

Keywords: Hand-held Raman spectrometer; SWIR excitation; SERS nanotags; limits of detection; hollow gold nanoshells; chalcogenopyrylium dyes

Main Text

Raman spectroscopy is an efficient and effective technique for identifying and distinguishing between materials.(1) It offers good molecular specificity and due to recent advancements in instrumentation, is regarded as a portable and easy to use technique.(2) In addition, there is little to no sample preparation required, it is non-contact and non-destructive and as such is currently being employed in a range of industries from pharmaceutical to counter-terrorism and from art to archeology.(1-5) Traditionally, Raman spectroscopy employed laser excitation wavelengths in the visible region because the intensity of Raman scattering is dependent on the 4^{th} power of the excitation frequency. Thus, the scattering effect is stronger at shorter wavelengths (532 nm - 785 nm). However, at visible excitation wavelengths problems can be encountered such as increased background fluorescence and sample degradation.(1) The number of molecules which fluoresce at shorter wavelengths is greater than at longer wavelengths. Hence, by moving to a short-wave infrared (SWIR) laser excitation between 950 and 1700 nm, fluorescence can be significantly reduced.(6-8) In addition, there is limited photobleaching and the infrared region provides an uncongested spectral window for optical analysis due to the absorption and scattering backgrounds of many molecules (in particular bio-molecules) being at a minimum.(9-12) In order to utilise these advantages, research focused on the design of Raman instruments operating at these longer wavelengths and instruments that are portable are of particular current interest.(6, 13)

As a result there has been an increase in the number of publications reporting the use of portable 1064 nm Raman spectrometers with the main areas of interest involving homeland security, forensic, bio-medical and geological applications.(2-4, 14, 15)

Raman scattering is significantly weaker in the infrared region than in the visible and as such weak signals are often obtained. Nonetheless, the poor signal response can be overcome by attaching or trapping molecules close to the surface of metallic nanoparticles, thus giving rise to the phenomenon known as surface enhanced Raman scattering (SERS).(1, 16) The intensity of scattering from SERS is dependent on coupling with the plasmon from the enhancing surface and can give intense signals well into the infrared.(17, 18) Enhancements of 10^6 have been reported, thus are several orders of magnitude greater than those reported for conventional Raman scattering.(19-21) Additional enhancements, up to 10^{14} can be achieved by tuning the laser frequency with an electronic transition within the analyte hence using a chromophore bound to a roughened metal surface to give rise to the phenomenon known as surface enhanced resonance Raman scattering (SERRS).(1) Therefore the SERRS enhancement is due to both surface plasmon resonance and molecular resonance and it allows for greater enhancement factors to be obtained while also improving the sensitivity and selectivity.(22)

SERS nanotags are *in situ* probes consisting of metallic nanoparticles and organic reporter molecules. They provide sensitive and selective analytical tools for studying chemical and biological systems.(23) Aggregated noble metal nanoparticles, commonly silver and gold are used as suspension based SERS substrates, as they are stable materials and have localised surface plasmon resonances (LSPR) that can be tuned from the visible to the infrared region by modifying the size, shape or surface chemistry.(23, 24) To date most of the research has focused on designing SERS nanotags for use with visible laser excitations but due to the benefits of operating in the SWIR region, research is emerging on the use of SERS combined with 1064 nm laser excitation and very recently with 1280 nm and 1550 nm.(25-30)

To coincide with advancements in instrumentation, it is vital to develop SERS nanotags that are capable of providing sensitive and reproducible responses in the uncongested spectral window of the infrared region while using a portable device. Up till now, the majority of publications have reported the use of FT-Raman spectrometers; however recently reports are emerging with the use of dispersive Raman instruments.(25-27) Although these instruments are technically classed as portable, they are bulky, heavy units which still require connection to a power supply and computer. Hand-held instruments on the other hand, are unique in that they are small, light, battery-operated (if required) and can be easily used by a single operator in diverse and challenging environments. We believe that a hand-held Raman spectrometer in combination with our unique chalcogenopyrylium nanotags could provide the portability and sensitivity required to combat the challenges currently being faced in the SWIR region, thus, could be pivotal for future advancements in homeland security, biological and clinical applications.

Herein, we report that hollow gold nanoshells (HGNs) modified with chalcogenopyrylium dyes give strong SERS responses with femtomolar detection limits being obtained using a hand-held 1064 nm Raman spectrometer. The Snowy Range CBEx Raman spectrometer is

regarded as hand-held, light-weight and portable as it has the following dimensions 4.5 x 3.125 x 2.25 inches, weighs 773g and can operate solely using four AA batteries. We have previously demonstrated the SERS capabilities of the chalcogenopyrylium dyes with HGNs and large gold nanoparticles; with picomolar (pM) detection limits being obtained using both 1280 nm and 1550 nm laser excitations.(28, 29) It was found that 2-thienyl and 2-selenophenyl substituents make excellent attachment groups for adsorbing strongly onto gold surfaces and the fine tuning of the absorbance maxima into the infrared region arises by interchanging the chalcogen atoms in the backbone and in the ring systems.

Specifically in this work, the SERS capabilities of HGNs functionalised with 17 different chalcogenopyrylium dyes (chalcogen nanotags) were investigated using a hand-held 1064 nm Raman spectrometer. It should be noted that an inorganic salt, specifically potassium chloride (KCl) was used to aggregate the nanotags as it increases the SERS signal by screening the Coloumbic repulsion energy between the nanoparticles allowing the reporter molecules to adhere more closely to the nanoparticle surface. We have previously shown that reproducible and stable nanotags (HGNs functionalised with a Raman reporter) can be prepared when 30 mM KCl is used as the aggregating agent.(28, 31) It was found at a concentration greater than 30 mM the HGNs precipitated out of solution and below this, weaker SERS signals were observed. Moreover, we demonstrated that by using this optimal concentration of KCl the LSPR of the HGNs did not shift but the enhancement in SERS signal was undeniable. Extinction spectroscopy, dynamic light scattering and zeta potential analysis were used previously to investigate the stability of the nanotags and it was found that for both the commercial reporter BPE (1,2-bis(4-pyridyl)ethylene) and chalcogenopyrylium dye 14, that upon adding the Raman reporter and aggregating with KCl, the LSPR of the HGNs did not shift nor was there broadening of the peak however slight dampening in the absorption maxima was observed. Further, a size increase and a decrease in zeta potential values indicated a change to the colloidal solution but ultimately it was concluded that the nanotags were stable and not over-aggregating.(28, 31) In addition, it is important to note that the plasmon resonance frequencies, hence LSPR of the HGNs (which is 710 nm, figure S1, ESI) does not need to match the excitation frequency of the laser for effective SERS to be achieved.(31-34) Therefore, by exploiting our previous knowledge SERS nanotags which are optimal for use in the SWIR region have been developed. Moreover, in this work the SERS response from chalcogen nanotags were compared to commercial reporters BPE and AZPY (4,4-azopyridine) also adsorbed onto the surface of HGNs and aggregated with 30 mM KCl. BPE and AZPY were chosen as they are non-resonant commercial reporters which have previously been exploited and shown to provide excellent SERS responses with HGNs and other SERS substrates at this laser wavelength.(31, 35-37)

Dyes 1-17 incorporate sulfur and selenium atoms in the chalcogenopyrylium core and, as previously mentioned, the 2-thienyl and 2-selenophenyl substituents on select members of this library provide unique attachment points for adsorbing onto the gold surface of the HGNs.(28) It has previously been reported that dye 14 binds to the HGN surface with a chalcogen tripod arrangement, essentially with two selenium atoms and one sulfur atom directly facing the gold surface.(17) SERS, SERRS, theoretical calculations and sum-frequency generation vibrational spectroscopy were all used to define the orientation and

manner of attachment. The study was very extensive in which the interpretation of the SE(R)RS spectra was thorough with each peak being assigned and the changes in the spectra (between the laser wavelengths) being explained in terms of the SERS effect. A study of this scale is not possible for all the nanotags tested herein, however general observations have been made and the results obtained support our previous findings.

It can be observed in figure 1 and figure S3 (ESI) that modification of the dye substituents alters the SERS spectrum significantly. The structures for each of the chalcogen dyes plus the commercial reporters are given in figure S2 (ESI). Dyes 1-17 are highly aromatic with absorbance maxima from 653 to 986 nm (table 1). The HGNs have a LSPR at 710 nm (figure S1, ESI) and it was found that the dyes attach strongly onto the surface of HGNs and as such produce vibrationally rich and intense SERS spectra using the 1064 nm laser excitation (figure 1 and S3, ESI). In general, the dyes which have absorption maxima closest to the laser excitation wavelength produced the best SERS signals but this was to be expected as contributions from both molecular resonance and surface enhancement would have led to the increased SERS response.(1) Experimental details on the SERS characterisation of the nanotags and synthetic scheme of the new chalcogenopyrylium dye 15 are provided in the materials and methods section with additional information being provided in the ESI.

Figures 1 and S3 (ESI), show the SERS spectra obtained when each of the reporter molecules at a concentration of 10 μM were added to the HGNs and analysed using a hand-held 1064 nm Raman spectrometer. All the measurements had a 0.05-1 second acquisition time and a laser power operating at 30 mW. It should be noted that the experimental set-up shown in schematic S1a (ESI) was employed in these studies. The experimental and instrumental parameters where kept constant throughout the analysis. In addition, Raman reporter and KCl stocks were freshly prepared daily. The solutions of each component (HGN, reporter, KCl) were tested separately as were the glass vials to ensure that no Raman signal was observed prior to analysis of the nanotag. Therefore eliminating the chance of contamination and confirming that the signal observed was solely due to the SERS active nanotags. It should be noted that the nanotags were compared based on their intensities. Therefore, when comparing the most intense peak at ~1600 cm^{-1} which arises due to heterocyclic aromatic ring stretching within the molecule;(17, 28, 36, 37) the pentamethine dyes (16 and 17) produced the strongest SERS response with the hand-held spectrometer, followed by the trimethine substituents, then the monomethine substituents and finally the commercial reporters produced the weakest SERS response. Generally, these results abide with the selection rules of SERRS; with the strongest signals being observed from the chalcogen dyes (dyes 16 and 17) which have absorption maxima closest to the laser frequency and the poorest signals being observed from the non-resonant commercial reporters. The SERRS effect alone however, could not be used to determine which nanotag would produce the best Raman signals as we have shown previously that the number of sp^2 carbons present in the chalcogenopyrylium backbone and functional groups used for binding to the HGN surface all have an effect on the signal.(28, 29)

When comparing BPE with the strongest chalcogen dye, a signal enhancement of approximately 60-fold was observed for dye 16 over the commercial reporter (figure 1). The

enhancement was even greater when comparing dye 16 to AZPY thus demonstrating the superiority of these chalcogen dyes as Raman reporters. It can also be seen that dye 16 produced a more intense SERS spectrum than dye 17 confirming that the selenolates have greater affinity to the gold surface of the HGNs than the thiolates. In general, it was observed that the selenophenes produced stronger SERS spectra than the sulfur substituents when comparing all the reporter molecules and this is consistent with our previous findings.(28, 29)

Pentamethine dyes, 16 and 17, produced the strongest SERS response but this was to be expected as we have previously demonstrated that increasing the number of sp^2 carbons in the chalcogenopyrylium backbone causes a significant red-shift in the absorption maximum and a resultant increase in the SERS signal. It is thought that by increasing the number of sp^2 carbons, that a greater displacement along the π-backbone will occur during the vibration, resulting in a greater polarisability and electromagnetic enhancement being experienced.(28) Hence for the pentamethine dyes, not only do they have unique S and Se attachment groups, they also have 5 sp^2 carbons in their backbone hence they demonstrate the most red-shifted absorption maxima (table 1). In fact, their wavelength maxima at 959 nm (dye 16) and 986 nm (dye 17) is very close to coinciding with the laser excitation and as such a contribution from both molecular resonance and surface enhancement is likely to have led to their exceptional SERS response. Furthermore, as shown in figure 1 and figure S3 (ESI), all 17 chalcogen dyes produced outstanding SERS signals with HGNs using the 1064 nm hand-held spectrometer. HGNs have previously been prepared with LSPRs upto 1320 nm and when synthesised with a shell thickness >9 nm they can be used as efficient SERS substrates.(31, 38, 39) Signal enhancements are observed when the surface plasmon resonance of the substrate matches that of the laser excitation, therefore the fact that the LSPR of the HGNs can be tuned from 500 to 1320 nm, we believe that these chalcogen nanotags could be designed to work with any laser excitation from the visible to the SWIR region. In addition, as previously mentioned the Raman signals obtained would be significantly enhanced through the SERRS effect, increasing the value and opportunities for the use of these nanotags. See table 1 for the absorption maximum (λ_{max}) values for the 17 chalcogenopyrylium dyes. Extinction spectra highlighting the wavelength maximum for a selection of the chalcogenopyrylium dyes are provided in figure S4.

Due to the remarkable SERS response obtained with the hand-held spectrometer, it was important to investigate the level of sensitivity which could be achieved; therefore particle dilution studies were conducted in order to determine limits of detection (LODs). Therefore, all 17 chalcogen dyes plus BPE and AZPY with HGNs were analysed over the concentration range 2 nM to 0.1 pM. It should be noted, that the nanoshells were initially mixed with a Raman reporter at a dye concentration of 10 μM before being diluted with deionised water to the required concentration. The initial particle concentration was 2 nM and subsequent dilutions were made until no signals from the nanotags were observed with the hand-held spectrometer. All experimental conditions were kept the same as those stated previously except an exposure time of 7 seconds was employed in this analysis. The peak at ~1600 cm^{-1} was used to calculate the LOD since it was the most intense peak in the spectrum. Figure 2 and figure S5 (ESI) show that a linear response was obtained for all the nanotags. The LOD was calculated to be 3 times the standard deviation of the blank, divided by the gradient of

the straight line which can be observed in each of the plots in figure 2 and figure S5 (ESI). Furthermore, table 1 lists the LOD values with associated standard deviation (s.d.) values for each of the chalcogen nanotags plus the LODs obtained for BPE and AZPY analysed using 1064 nm laser excitations.

The pentamethine dyes 16 and 17 produced the best results with extremely low values of 4.6 ± 0.34 fM and 4.8 ± 0.37 fM, respectively. Trimethine dyes 9-15 had LODs from 0.1 to 1.0 pM, while the monomethine dyes 1-8 had LODs from 0.5 to 1.1 pM. However, the commercially available reporters gave the highest LOD values at 0.15 and 0.19 nM for AZPY and BPE respectively. These are 2-to-3 orders of magnitude higher than the monomethine and trimethine chalcogenopyrylium dyes and 4-to-5 orders of magnitude higher than the pentamethine chalcogenopyrylium dyes. This demonstrates the superiority of these chalcogenopyrylium nanotags for use with this SWIR laser excitation. Furthermore, all 17 of the chalcogen nanotags were shown to have a LOD value at least one order of magnitude below the commercial ones, with values ranging from 1.1 pM to 4.6 fM. The sensitivity which has been achieved at this laser excitation wavelength is exceptional, however the fact the results were also obtained using a hand-held spectrometer is unprecedented. These unique nanotags are capable of providing strong SERS signals in the biological window of the SWIR region but the fact that they provide ultra-low sensitivity with a hand-held device means that these results could provide the basis for future advancements in bio-medical and optical applications.

Conclusions

In conclusion, we have demonstrated that femtomolar sensitivity can be achieved using a hand-held Raman spectrometer incorporating a 1064 nm laser excitation. The combination of chalcogenopyrylium dyes plus HGNs make ideal SERS nanotags for operating in the SWIR region. These unique tags have demonstrated detection limits two-to-five orders of magnitude lower than the commercially available ones. In addition, the fact their LSPRs can be tuned well into the infrared making them flexible across a range of laser wavelengths. Hence, the combination of these chalcogen nanotags plus a hand-held instrument, make for great advancements in terms of the portability and sensitivity required for future applications in homeland security, food safety and bio-medical analysis.

Materials and Methods

With the exception of dye 15, dyes 1-17 were synthesised as reported in previous publications by Bedics and Kearns *et al.*(28, 29) Additionally, the synthetic procedure for HGNs was also detailed in these publications.

Dye 15 [4-(3-(2,6-diphenyl-4H-thiopyran-4-ylidene)prop-1-enyl)-2-phenylselenobenzo-pyrylium hexafluorophosphate] is new to this subset of chalcogenopyrylium dyes and as such the synthesis scheme is provided below (scheme 1) with the experimental detail for the synthesis and characterisation of this dye along with dyes 16 and 17 being provided in the supporting information (ESI).

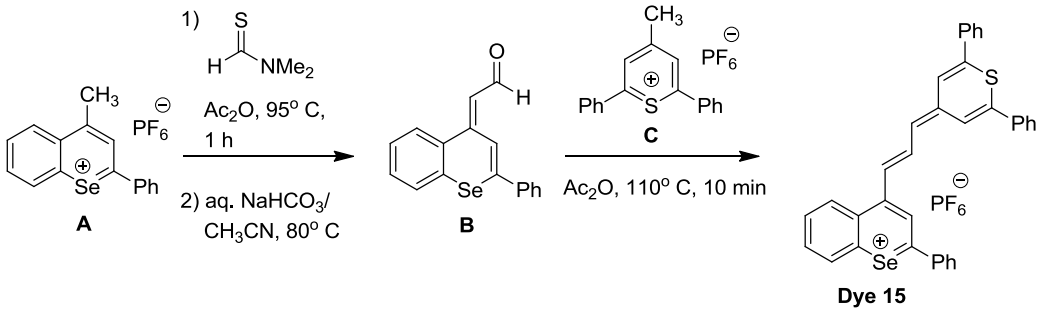

Scheme 1. Synthesis of Dye 15.

SERS Characterisation

Investigation into the properties of the SERS nanotags were carried out by mixing 'as-prepared' HGN solution (270 µL; 2.8 nM) with Raman reporter solution (40 µL, 10 µM) and potassium chloride (300 µL; 30 mM). At this excitation wavelength 19 Raman reporters were analysed, two of which where the commercial reporters BPE and AZPY for comparison. The structures of all Raman reporters analysed can be seen in figure S2. The SERS measurements were performed using a hand-held Snowy Range 'CBEx' Raman spectrometer (Laramie, USA) with a diode laser operating at 1064 nm excitation wavelength. The portable spectrometer has the following dimensions 4.5 x 3.125 x 2.25 inches (114 x 79 x 57 mm) and weighs just 773 g (27 oz). It should be noted that experimental setup a) was employed in this analysis (schematic S1). All the measurements had a 0.05-1 second acquisition time and a laser power operating at 30 mW. Each sample was prepared in triplicate and 5 scans of each replicate were recorded. All the Raman spectra were background corrected using a multi-point linear fit and level and zero-levelling mode in Grams software (AI 7.0).

For the SERS particle dilution studies, the optimum conditions were initially used (as stated above) and deionised water was added to obtain subsequent concentrations, over the concentration range of 2 nM to 0.1 pM. All other experimental conditions were kept the same as those stated above except an exposure time of 7 seconds was employed in this analysis. The limit of detection (LOD) was calculated to be 3 times the standard deviation of the blank, divided by the gradient of the straight line. Error bars represent one standard deviation resulting from 3 replicate samples and 5 scans of each, see table 1 for the LOD values for chalcogen dyes 1-17 plus BPE and AZPY adsorbed onto HGNs and figure S5 for associated LOD plots with error bars for dyes 1-15, 17 and AZPY.

A schematic detailing the experimental setup (schematic S1) plus additional information regarding the preparation of the nanotags are provided in the ESI.

Ethics statement

This does not apply to the manuscript.

Data accessibility

Electronic supplementary information (ESI) available: General experimental details for the synthesis and characterisation of dyes 1-17 and HGNs; schematic detailing experimental setup, figures of extinction spectra for HGNs and selected chalcogenopyrylium dyes; chemical structures for dyes 1-17 and commercial reporters; SERS spectra and LOD plots for dye/HGN nanotags plus commercial reporter/HGN nanotags with 1064 nm excitation.

The research data associated with this paper will become available at the following link: http://dx.doi.org/10.15129/11368265-f134-4d8b-91d1-0e9b916e7c12

Author's contributions

HK carried out lab work, participated in data and statistical analysis, participated in the design and coordination of the study and drafted the manuscript; FA carried out lab work and participated in data analysis; MB synthesised and characterised the dyes; NS, KF and MD helped coordinate the study and critically reviewed the manuscript, DG participated in the design and coordination of the study and critically reviewed the manuscript. All authors gave final approval for publication.

Competing interests

The authors declare no competing financial interests.

Funding

This work was supported by the Royal Society in the form of a Wolfson Research Merit Award, Defence Science and Technology Laboratory (Dstl), Engineering and Physical Sciences Research Council [grant number EP/J500550/1] and the National Science Foundation [grant CHE-1151379].

Acknowledgements

The authors would like to thank all funders who supported this work and are very grateful to the two anonymous reviewers who provided comments that substantially improved this manuscript.

Figures

Table 1 - Values of the absorption maximum (λ_{max}) and calculated LOD values from the SERS experiment with associated standard deviation (s.d.) error for 17 chalcogenopyrylium dyes plus BPE and AZPY adsorbed onto HGNs using a hand-held 1064 nm Raman spectrometer.

Dye	**λ_{max} nm (CH_2Cl_2)**	**1064 nm LOD, pM[a]**	**Structure Type**
1	653	0.7 ± 0.07	Monomethine dyes
2	676	0.8 ± 0.08	
3	699	0.7 ± 0.10	
4	676	1.0 ± 0.12	
5	698	0.6 ± 0.05	
6	723	1.1 ± 0.16	
7	659	0.6 ± 0.05	
8	687	0.5 ± 0.08	
9	806	0.6 ± 0.05	Trimethine dyes
10	784	0.3 ± 0.03	
11	810	0.3 ± 0.02	
12	789	0.3 ± 0.02	
13	813	0.2 ± 0.02	
14	826	0.1 ± 0.01	
15	748	1.0 ± 0.12	
16	959	4.6 ± 0.34 fM*	Pentamethine dyes
17	986	4.8 ± 0.37 fM*	
18 - **AZPY**	Non-resonant	0.15 ± 0.02 nM*	Commercial reporters
19 – **BPE**	Non-resonant	0.19 ± 0.02 nM*	

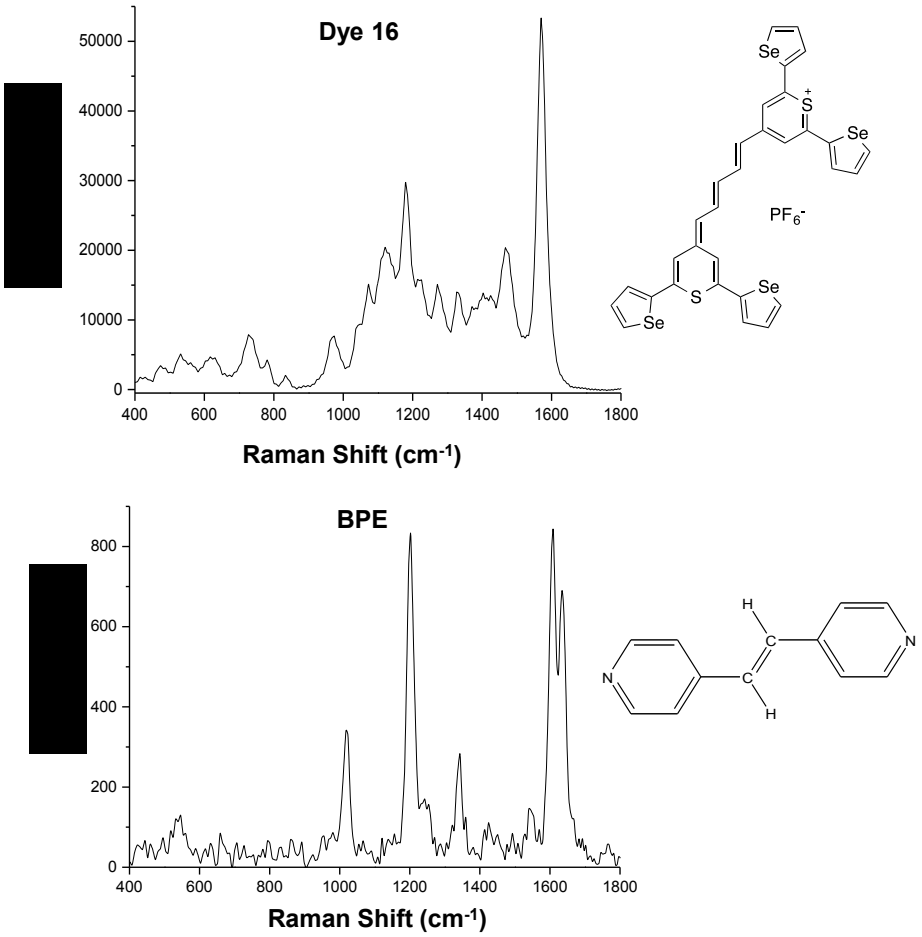

Figure 1 – Comparison of SERS spectra for chalcogenopyrylium dye 16 with the commercial Raman reporter BPE. The dyes with a concentration of 10 μM were analysed with HGNs (SPR recorded at 710 nm, figure S1, ESI) and KCl. A laser excitation of 1064 nm was employed in this analysis with an exposure time of 0.05 seconds for the chalcogen dye 16 and 1 second for the commercial reporter BPE. All spectra have been background corrected.

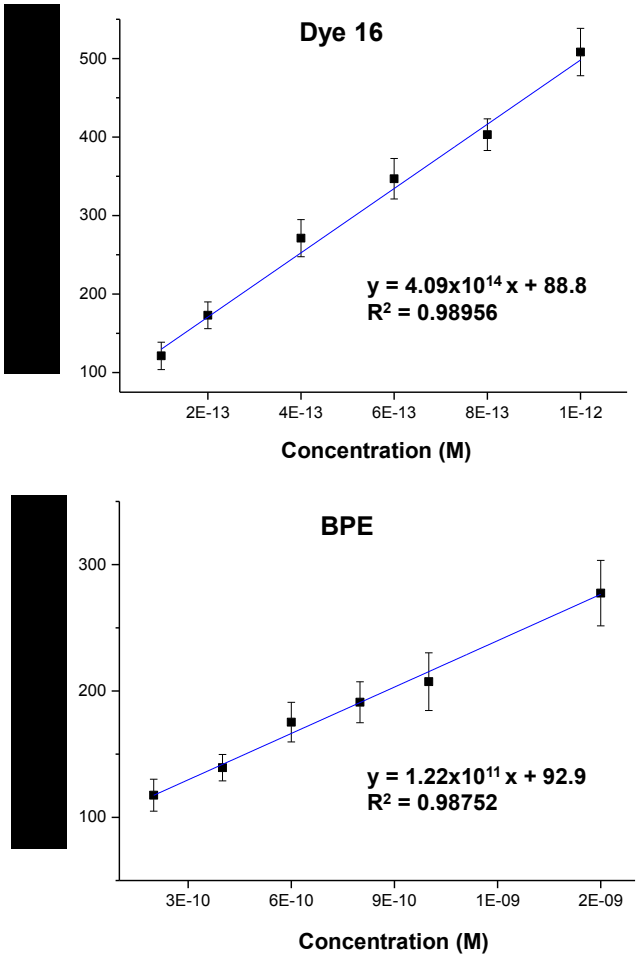

Figure 2 - SERS particle dilution studies for chalcogenopyrylium dye 16 plus commercial Raman reporter BPE with HGNs and KCl over the concentration range 2 nM to 0.1 pM. A laser excitation of 1064 nm and an exposure time of 7 seconds were employed in this analysis. Error bars represent one standard deviation resulting from 3 replicate samples and 5 scans of each.

References

1. Smith E, Dent G, Wiley J. Modern Raman spectroscopy: a practical approach: Wiley Online Library; 2005.
2. Izake EL. Forensic and homeland security applications of modern portable Raman spectroscopy. Forensic Science International. 2010;**202**(1):1-8 (doi:10.1016/j.forsciint.2010.03.020).
3. Vítek P, Ali EM, Edwards HG, Jehlička J, Cox R, Page K. Evaluation of portable Raman spectrometer with 1064nm excitation for geological and forensic applications. Spectrochimica Acta Part A: Molecular and Biomolecular Spectroscopy. 2012;**86**:320-7 (doi:10.1016/j.saa.2011.10.043).
4. Vítek P, Jehlička J, Edwards HG, Hutchinson I, Ascaso C, Wierzchos J. The miniaturized Raman system and detection of traces of life in halite from the Atacama Desert: some considerations for the search for life signatures on Mars. Astrobiology. 2012;**12**(12):1095-9 (doi:10.1089/ast.2012.0879).

5. Sorak D, Herberholz L, Iwascek S, Altinpinar S, Pfeifer F, Siesler HW. New developments and applications of handheld Raman, mid-infrared, and near-infrared spectrometers. Applied Spectroscopy Reviews. 2012;**47**(2):83-115 (doi:10.1080/05704928.2011.625748).

6. Lynn KA, McNay G, Eustace DA, Shand NC, Smith WE. Short-wave infrared excited SERS. Analyst. 2010;**135**(8):1904-5 (doi:10.1039/C0AN00096E).

7. Donahue M, Huang H, Brouillette C, Smith W, Farquharson S. Detecting Explosives by Portable Raman Analyzers: A Comparison of 785-, 976-, 1064-, and 1550-nm (Retina-Safe) Laser Excitation. Spectroscopy Onlinecom. 2011, Accessed April 2017, (http://www.spectroscopyonline.com/detecting-explosives-portable-raman-analyzers-comparison-785-976-1064-and-1550-nm-retina-safe-laser).

8. Asselin KJ, Chase B. FT-Raman spectroscopy at 1.339 micrometers. Applied Spectroscopy. 1994;**48**(6):699-701 (doi:10.1366/000370294774369009).

9. Anderson RR, Parrish JA. The optics of human skin. Journal of Investigative Dermatology. 1981;**77**(1):13-9 (doi:10.1111/1523-1747.ep12479191).

10. Bashkatov A, Genina E, Kochubey V, Tuchin V. Optical properties of human skin, subcutaneous and mucous tissues in the wavelength range from 400 to 2000 nm. Journal of Physics D: Applied Physics. 2005;**38**(15):2543 (doi:10.1088/0022-3727/38/15/004).

11. Culha M, Cullum B, Lavrik N, Klutse CK. Surface-enhanced Raman scattering as an emerging characterization and detection technique. Journal of Nanotechnology. 2012;**2012**:1-15 (doi:10.1155/2012/971380).

12. Chen IH, Chu SW, Sun CK, Cheng PC, Lin BL. Wavelength dependent damage in biological multi-photon confocal microscopy: A micro-spectroscopic comparison between femtosecond Ti: sapphire and Cr: forsterite laser sources. Optical and Quantum Electronics. 2002;**34**(12):1251-66 (doi:10.1023/A:1021303426482).

13. Brouillette C, Huang H, Smith W, Farquharson S. Raman Spectroscopy Using 1550 nm (Retina-Safe) Laser Excitation. Applied Spectroscopy. 2011;**65**(5):561-3, Accessed April 2017 (www.osapublishing.org/as/abstract.cfm?uri=as-65-5-561).

14. Roy E, Wilcox PG, Hoffland S, Pardoe I, editors. Detection of munitions grade g-series nerve agents using Raman excitation at 1064 nm. Proceeds of SPIE Security + Defence: International Society for Optics and Photonics. 2015;**965202** (doi:10.1117/12.2194027).

15. Jehlička J, Edwards HG, Oren A. Raman spectroscopy of microbial pigments. Applied and Environmental Microbiology. 2014;**80**(11):3286-95 (doi:10.1128/AEM.00699-14).

16. Wang Y, Schlücker S. Rational design and synthesis of SERS labels. Analyst. 2013;**138**(8):2224-38 (doi:10.1039/C3AN36866A).

17. Kearns H, Sengupta S, Sasselli IR, Bromley III L, Faulds K, Tuttle T, Bedics MA, Detty MR, Velarde L, Graham D, Smith WE. Elucidation of the bonding of a near infrared dye to hollow gold nanospheres–a chalcogen tripod. Chemical Science. 2016**;7**:5160-70 (doi:10.1039/c6sc00068a).

18. Liang E, Engert C, Kiefer W. Surface- enhanced Raman scattering of pyridine in silver colloids excited in the near- infrared region. Journal of Raman Spectroscopy. 1993;**24**(11):775-9 (doi:10.1002/jrs.1250241109).

19. Fleischmann M, Hendra PJ, McQuillan A. Raman spectra of pyridine adsorbed at a silver electrode. Chemical Physics Letters. 1974;**26**(2):163-6 (doi:10.1016/0009-2614(74)85388-1).

20. Jeanmaire DL, Van Duyne RP. Surface Raman spectroelectrochemistry: Part I. Heterocyclic, aromatic, and aliphatic amines adsorbed on the anodized silver electrode. Journal of Electroanalytical Chemistry and Interfacial Electrochemistry. 1977;**84**(1):1-20 (doi:10.1016/0009-2614(74)85388-1).

21. Albrecht MG, Creighton JA. Anomalously intense Raman spectra of pyridine at a silver electrode. Journal of the American Chemical Society. 1977;**99**(15):5215-7 (doi:10.1021/ja00457a071).

22. Graham D, Smith WE, Linacre AM, Munro CH, Watson ND, White PC. Selective detection of deoxyribonucleic acid at ultralow concentrations by SERRS. Analytical Chemistry. 1997;**69**(22):4703-7 (doi:10.1021/ac970657b).

23. Harper MM, McKeating KS, Faulds K. Recent developments and future directions in SERS for bioanalysis. Physical Chemistry Chemical Physics. 2013;**15**(15):5312-28 (doi:10.1039/C2CP43859C).

24. Qian XM, Nie S. Single-molecule and single-nanoparticle SERS: from fundamental mechanisms to biomedical applications. Chemical Society Reviews. 2008;**37**(5):912-20 (doi:10.1039/B708839F).

25. Oldenburg SJ, Westcott SL, Averitt RD, Halas NJ. Surface enhanced Raman scattering in the near infrared using metal nanoshell substrates. The Journal of Chemical Physics. 1999;**111**(10):4729-35 (doi:10.1063/1.479235).

26. Wijesuriya S, Burugapalli K, Mackay R, Ajaezi GC, Balachandran W. Chemically roughened solid silver: A simple, robust and broadband SERS substrate. Sensors. 2016;**16**(10):1742 (doi:10.3390/s16101742).

27. Gühlke M, Heiner Z, Kneipp J. Combined near-infrared excited SEHRS and SERS spectra of pH sensors using silver nanostructures. Physical Chemistry Chemical Physics. 2015;17(39):26093-100 (doi:10.1039/C5CP03844H).

28. Bedics MA, Kearns H, Cox JM, Mabbott S, Ali F, Shand NC, Faulds K, Beneduct JB, Graham D, Detty MR. Extreme Red Shifted SERS Nanotags. Chemical Science. 2015;**6**:2302-6 (doi:10.1039/C4SC03917C).

29. Kearns H, Bedics MA, Shand NC, Faulds K, Detty MR, Graham D. Sensitive SERS nanotags for use with 1550 nm (retina-safe) laser excitation. Analyst. 2016;**141**(17):5062-5 (doi:10.1039/C5AN02662H).

30. Milojevich CB, Mandrell BK, Turley HK, Iberi V, Best MD, Camden JP. Surface-enhanced hyper-Raman scattering from single molecules. The Journal of Physical Chemistry Letters. 2013;**4**(20):3420-3 (doi:10.1021/jz4017415).

31. Kearns H, Shand N, Smith W, Faulds K, Graham D. 1064 nm SERS of NIR active hollow gold nanotags. Physical Chemistry Chemical Physics. 2015;**17**:1980-6 (doi:10.1039/C4CP04281F).

32. Kleinman SL, Ringe E, Valley N, Wustholz KL, Phillips E, Scheidt KA, Schatz GC, Van Duyne RP. Single-Molecule Surface-Enhanced Raman Spectroscopy of Crystal Violet Isotopologues: Theory and Experiment. Journal of American Chemical Society. 2011;**133**(11):4115-2 (doi:10.1021/ja110964d).

33. Abalde- Cela S, Ho S, Rodríguez- González B, Correa- Duarte MA, Álvarez- Puebla RA, Liz- Marzán LM, Kotov NA. Loading of exponentially grown LBL films with silver nanoparticles and their application to generalized SERS detection. Angewandte Chemie. 2009;**121**(29):5430-3 (doi:10.1002/anie.200901807).

34. Nikoobakht B, Wang J, El-Sayed MA. Surface-enhanced Raman scattering of molecules adsorbed on gold nanorods: off-surface plasmon resonance condition. Chemical Physics Letters. 2002;**366**(1):17-23 (doi:10.1016/S0009-2614(02)01492-6).

35. Xie H, Larmour IA, Chen YC, Wark AW, Tileli V, McComb DW, Faulds K, Graham D. Synthesis and NIR optical properties of hollow gold nanospheres with LSPR greater than one micrometer. Nanoscale. 2013;**5**(2):765-71 (doi:10.1039/C2NR33187J).

36. Zhuang Z, Shang X, Wang X, Ruan W, Zhao B. Density functional theory study on surface-enhanced Raman scattering of 4, 4′-azopyridine on silver. Spectrochimica Acta Part A: Molecular and Biomolecular Spectroscopy. 2009;**72**(5):954-8 (doi:10.1016/j.saa.2008.12.027).

37. Zhuang Z, Shi X, Chen Y, Zuo M. Surface-enhanced Raman scattering of trans-1, 2-bis (4-pyridyl)-ethylene on silver by theory calculations. Spectrochimica Acta Part A: Molecular and Biomolecular Spectroscopy. 2011;**79**(5):1593-9 (doi:10.1016/j.saa.2011.05.017).

38. Xie H, Larmour IA, Smith WE, Faulds K, Graham D. Surface-Enhanced Raman Scattering Investigation of Hollow Gold Nanospheres. The Journal of Physical Chemistry C. 2012:**116**:8338–42 (doi:10.1021/jp3014089).

39. Schwartzberg AM, Olson TY, Talley CE, Zhang JZ. Synthesis, Characterization, and Tunable Optical Properties of Hollow Gold Nanospheres. The Journal of Physical Chemistry B. 2006;**110(**40):19935-44 (doi:10.1021/jp062136a).